

We substitute Eq. (3.15) into (A10), and derive the relation

$$\epsilon_1^\pm(\omega) = \hat{L}(\omega - E^0 \mp \lambda)$$

$$\hat{L}(\omega - E^0) = -P \int_1^\infty \frac{L(\omega' - E^0)}{\omega' - \omega} d\omega'. \quad (\text{A16})$$

Thus, we have

$$\hat{W}_3 = \sqrt{\frac{3}{2}} D_3^3 (\epsilon_1^+ - \epsilon_1^-) / \lambda \quad (\text{A17})$$

in exact analogy to Eq. (3.18) for  $W_3$ .

However, we cannot now proceed to the analogous relation for  $Q_3$  without making a further approximation. We must assume that the structure in the reflectivity is small compared to the reflectivity itself, so that we can use Eq. (A2) to write

$$R^\pm / R = \alpha \epsilon_1^\pm + \beta \epsilon_2^\pm. \quad (\text{A18})$$

Equation (A18) then allows us to write

$$Q_3 = \sqrt{\frac{3}{2}} D_3^3 (R^+ - R^-) / \lambda R. \quad (\text{A19})$$

The accuracy of (A18) can be tested using results from Kramers-Kronig analyses on the unstrained reflectivity.

Our principal results are Eqs. (A7), (A9), (A15), and (A19) which are in exact analogy to Eqs. (3.4), (3.20), (3.17), and (3.18) for the  $W_j$ 's. Note that (A7) and (A9) for the  $Q_j$ 's are as accurate as the corresponding equations for the  $W_j$ 's. Equation (A15) requires an approximation which should generally be quite good. Equation (A19) requires a further approximation which is less accurate but can be checked if  $\epsilon_1$  and  $\epsilon_2$  are known for the unstrained crystal. Alternatively, one can use the relationship

$$Q_3 = \sqrt{\frac{3}{2}} (D_3^3 / \lambda) [\alpha (\epsilon_1^+ - \epsilon_1^-) + \beta (\epsilon_2^+ - \epsilon_2^-)]. \quad (\text{A20})$$

Equation (A20) is much more accurate than (A19), and should compare to (A15) in accuracy. The only approximation required to derive (A20) from (3.18) was the neglect of the nonresonant denominator in Eq. (A4) as in Eq. (A10). If  $\epsilon_2^\pm$  has been determined, Eqs. (A16) specify  $\epsilon_1^\pm$ .

## Observation of Mixed-Mode Excitons in the Photoluminescence of Zinc Oxide

R. L. WEIHER AND W. C. TAIT

3M Company, Central Research Laboratories, St. Paul, Minnesota 55101

(Received 26 March 1969)

Mixed-mode excitons have been previously reported in the absorption spectrum of uniaxial II-VI crystals when plane-polarized light is used with its  $\mathbf{E}$  field in a plane containing both the photon's wave vector  $\mathbf{k}$  and the  $c$  axis of the crystal. Lines due to annihilation of mixed-mode excitons should also be observed in the emission spectrum of these uniaxial crystals. We describe here the observation of such emission lines in the photoluminescence of ZnO at 77°K. The strengths of these lines are essentially zero when  $\mathbf{k} \perp c$ , but increase rapidly as the angle between  $\mathbf{k}$  and  $c$  is reduced below 90°. The energies of the  $A$  and  $B$  longitudinal excitons in Thomas's line assignment are found to be 3.373 and 3.386 eV, respectively, in good agreement with results obtained from reflectivity data.

IT has been shown theoretically by Hopfield and Thomas<sup>1</sup> that "longitudinal" excitons should be optically observable in uniaxial crystals. In that same paper, they demonstrated the existence of longitudinal excitons in ZnO by optical-absorption measurements. Similar observations have been made on CdS by Hopfield and Thomas<sup>2</sup> and on CdSe by Parsons, Wardzynski, and Yoffe<sup>3</sup> and by Wheeler and Dimmock,<sup>4</sup> as well as by other investigators.

The actual absorption lines observed are due to "mixed-mode" excitons which have components of both transverse and longitudinal polarizations. As shown by Hopfield and Thomas,<sup>1</sup> mixed-mode excitons are observed only when the light is polarized with the

electric field ( $\mathbf{E}$ ) in a plane containing both the photon propagation vector ( $\mathbf{k}$ ) and the  $c$  axis with the  $\mathbf{k}$  vector at some internal angle  $\phi$ , after refraction, with the  $c$  axis as shown in Fig. 1. When the angle  $\phi$  is 0° ( $\mathbf{k} \parallel c$ ), the excitons are pure transverse, and when  $\phi = 90^\circ$  ( $\mathbf{k} \perp c$ ), they are pure longitudinal. At all other angles, mixed-mode excitons are observed.

Two notable features of the mixed-mode excitons are the dependences of their oscillator strength and their position in energy on the angle  $\phi$ . The oscillator strength of the mixed mode is given by<sup>1</sup>

$$4\pi\beta_{\text{mx}} = 4\pi\beta_T \cos^2\phi, \quad (1)$$

where  $4\pi\beta_T$  is the oscillator strength of the transverse mode. The position, in energy, of the mixed mode is<sup>1</sup>

$$E_{\text{mx}} = E_T [1 + (4\pi\beta_T / \epsilon) \sin^2\phi]^{1/2}, \quad (2)$$

where  $E_T$  is the energy of the transverse mode and  $\epsilon$  is the dielectric constant due to all higher energy transitions.

<sup>1</sup> J. J. Hopfield and D. G. Thomas, *J. Phys. Chem. Solids* **12**, 276 (1960).

<sup>2</sup> J. J. Hopfield and D. G. Thomas, *Phys. Rev.* **122**, 35 (1961).

<sup>3</sup> R. B. Parsons, W. Wardzynski, and A. D. Yoffe, *Proc. Roy. Soc. (London)* **A262**, 120 (1961).

<sup>4</sup> R. G. Wheeler and J. O. Dimmock, *Phys. Rev.* **125**, 1805 (1962).

TABLE I. Emission maxima of various excitons.

Emission band	Position		Assignment
	(Å)	$E$ (eV)	
$B_T$	3669.6	3.378	Transverse $B$ exciton (in the notation of Thomas <sup>a</sup> )
$A_T$	3677.0	3.371	Transverse $A$ exciton (in the notation of Thomas <sup>a</sup> )
$\beta$	3680.0	3.369	Unknown
$I$	3688.7	3.361	Bound (extrinsic) exciton
$I'$	3692.7	3.357	Bound (extrinsic) exciton
$I''$	3696.7	3.353	Bound (extrinsic) exciton
$A_T - \hbar\omega$	3747.0	3.308	LO-phonon-assisted transverse $A$ exciton
$A_{mx}$	3675.2	3.373	Mixed-mode $A$ exciton (in the notation of Thomas <sup>a</sup> )
$B_{mx}$	3660.9	3.386	Mixed-mode $B$ exciton (in the notation of Thomas <sup>a</sup> )

<sup>a</sup> Reference 5.

Emission lines due to annihilation of mixed-mode excitons should also be described by Eqs. (1) and (2). We have observed such emission lines in the photoluminescence of ZnO that are unobservable  $\mathbf{E} \parallel c$ , but as the crystal was rotated about an axis perpendicular to the  $c$  axis, emission lines appeared at energies slightly above those of the transverse modes. The strengths of these lines increased as the angle between  $\mathbf{k}$  and the  $c$  axis decreased. It is the purpose of this note to report and discuss these observations.

The two lowest-lying transverse excitons ( $A_T$  and  $B_T$  in the notation of Thomas<sup>5</sup>) are seen in the emission spectrum of ZnO at 77°K, excited with uv, when  $\mathbf{E} \perp c$ ,  $\mathbf{k} \perp c$  as shown in Fig. 2(a). The transverse exciton  $A_T$  occurs at 3.371 eV, and  $B_T$ , although seen only as a shoulder on the high-energy side of the  $A_T$  emission band, is believed to occur near 3.378 eV. The other emission maxima seen in this polarization have been previously assigned,<sup>6</sup> as shown in Table I. Higher-order phonon replicas of the  $A_T - \hbar\omega$  band are also seen at lower photon energies, but are not shown in Fig. 2(a). No emission could be recorded for  $\mathbf{E} \parallel c$ ,  $\mathbf{k} \perp c$  when the crystal was properly aligned, and the entrance of the monochromator was apertured to accept radiation less than a degree from an axis normal to the crystal face.

Although the spectrum shown in Fig. 2(a) is in close agreement with that previously reported,<sup>6</sup> there exists a notable difference with that recently reported by Filinski and Skettrup.<sup>7</sup> They reported an emission maximum at 3.3729 eV for both  $\mathbf{E} \perp c$  and  $\mathbf{E} \parallel c$  and concluded that this maximum as well as the one near 3.371 eV were extrinsic in behavior. We observe this emission maximum in the mixed-mode geometry. No emission could be observed at  $\phi = 90^\circ$  ( $\mathbf{E} \parallel c$ ,  $\mathbf{k} \perp c$ ); however, as the crystal was rotated around an axis perpendicular to the  $c$  axis, emission lines appeared and grew in intensity as the angle between  $\mathbf{k}$  and the  $c$  axis became smaller.

<sup>5</sup> D. G. Thomas, J. Phys. Chem. Solids **15**, 86 (1960).

<sup>6</sup> R. L. Weiher and W. C. Tait, Phys. Rev. **166**, 791 (1968).

<sup>7</sup> I. Filinski and T. Skettrup, Solid State Commun. **6**, 233 (1968).

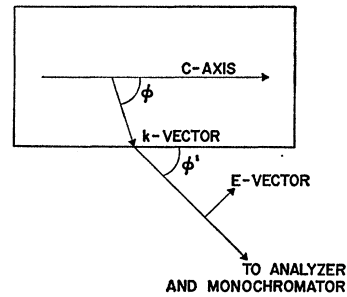


FIG. 1. Experimental geometry used in recording emission spectra of mixed-mode excitons. The  $\mathbf{E}$  vector of mixed mode is in the plane defined by  $\mathbf{k}$  and the  $c$  axis.

A typical emission spectrum for the mixed-mode geometry is shown in Fig. 2(b) for an external angle  $\phi'$  of  $67^\circ$  between  $\mathbf{k}$  and the  $c$  axis.<sup>8</sup> The emission spectrum for  $\mathbf{E} \perp c$  in this geometry, as well as for other angles, was identical to that shown in Fig. 2(a) for  $\mathbf{k} \perp c$ . The notable emission bands, designated  $A_{mx}$  and  $B_{mx}$ , seen only in the mixed-mode geometry, occur at 3.373 and 3.386 eV, respectively. It is seen that the energies of these emission bands occur slightly above those of the respective transverse modes and are in good agreement with  $A_{mx} = 3.373$  eV and  $B_{mx} = 3.389$  eV calculated from Eq. (2) for an internal angle ( $\phi$ ) near  $90^\circ$ . The shape and position of line  $A_{mx}$  was independent of the angle to approximately  $30^\circ$  (limit of measurements  $90^\circ - 30^\circ$ ). The line  $B_{mx}$  did appear to shift slightly to lower energy as the external angle was varied from  $90^\circ$  to  $30^\circ$ , but it also broadened and became merely a shoulder on the high-energy side of

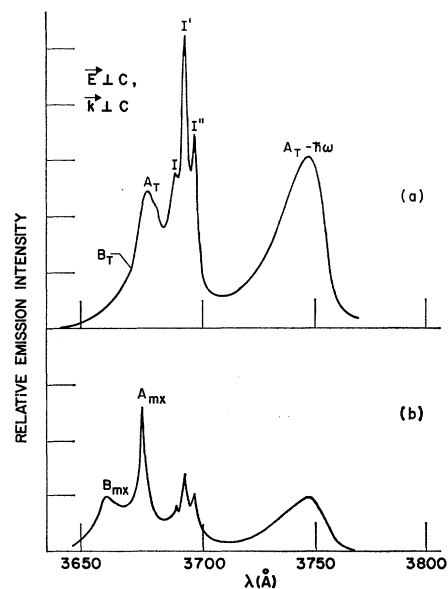


FIG. 2. (a) Photoluminescence of ZnO at 77°K for  $\mathbf{E} \perp c$ ,  $\mathbf{k} \perp c$ . (b) Photoluminescence of ZnO at 77°K for the mixed-mode geometry. This spectrum was obtained for an external angle  $\phi'$  of  $67^\circ$  between  $\mathbf{k}$  and the  $c$  axis.

<sup>8</sup> The internal angle  $\phi$  is, of course, much nearer to  $90^\circ$  because of refraction.

line  $A_{mx}$ , so that the exact shift could not be ascertained.

It is interesting to compare the emission spectrum for  $\mathbf{E} \perp c$  [Fig. 2(a)] and for the mixed-mode geometry [Fig. 2(b)]. In Fig. 2(a), the bound exciton lines ( $I$ ,  $I'$ , and  $I''$ ) dominate the spectrum. Because a small component of the  $\mathbf{E}$  vector can be resolved perpendicular to  $\mathbf{k}$  in the mixed-mode geometry, the bound excitons should be observed in this geometry if they are also dipole-allowed transitions. The oscillator strengths of the bound excitons should depend upon  $\phi$ , as given by Eq. (1). Also, because the reported refractive index<sup>9</sup> is larger near  $A_{mx}$  than the bound  $I$  lines, the refraction should be less near the  $I$  lines, so that these latter lines should consequently dominate the spectrum in Fig. 2(b). It is seen, however, that this is not the case. We believe that spatial dispersion effects may be responsible for the above unexpected behavior. It has been shown that the scattering of polaritons (apparent absorption) by phonons is dependent upon the shape of the polariton dispersion ( $\mathbf{E}$  versus  $\mathbf{k}$ ) curve.<sup>10,11</sup> Conversely, the contribution to the emission from the scattering of polaritons is expected to depend upon the shape of the dispersion curve especially just above the "knee" in the lower branch.<sup>12</sup> The knee occurs very near the crossing of the uncoupled exciton-photon dispersion curves, and it is at precisely this energy that the shape

of the polariton dispersion curve is the most sensitive to the coupling parameter  $4\pi\beta$ . It may be expected, then, that the emission due to intrinsic excitons (polaritons) would have some implicit nonlinear dependence on  $4\pi\beta_{mx}$ , given by Eq. (1).<sup>13</sup>

In conclusion, emission lines have been observed in ZnO which clearly verify the existence of mixed-mode excitons in photoluminescence. Mixed-mode excitons are observed for the two lowest-lying excitons ( $A$  and  $B$ ). This work points out the importance of precise alignment of uniaxial crystals when emission is measured for the polarization  $\mathbf{E} \parallel c$ ,  $\mathbf{k} \perp c$ . It seems likely that a slight sample misalignment would account for the observations and polarization assignments recently reported for some of the emission lines in ZnO by Filinski and Skettrup.<sup>7</sup> Recent emission studies<sup>7,14,15</sup> have again pointed out the controversy over the valence-band assignments in ZnO suggested by Thomas<sup>5</sup> and by Park *et al.*<sup>16</sup> The observations made in this note are in agreement with the assignment of Thomas,<sup>5</sup> and because of the noted difference in behavior between intrinsic and extrinsic excitons, a further study may provide conclusive proof of intrinsic or extrinsic nature.

We wish to thank G. Voll for experimental assistance.

<sup>13</sup> Mixed-mode excitons have also been observed in our laboratory in the emission spectrum of CdS crystals at different external angles  $\phi'$ . The intensity of the "free"  $A$  exciton-mixed-mode line in CdS has a similar dependence on  $\phi'$  as the  $A_{mx}$  line in ZnO.

<sup>14</sup> T. Skettrup and L. R. Lidholt, *Solid State Commun.* **6**, 589 (1968).

<sup>15</sup> C. Solbrig, *Z. Physik* **211**, 429 (1968).

<sup>16</sup> Y. S. Park, C. W. Litton, T. C. Collins, and D. C. Reynolds, *Phys. Rev.* **143**, 512 (1966).

<sup>9</sup> Y. S. Park and J. R. Schenider, *J. Appl. Phys.* **39**, 3049 (1968).

<sup>10</sup> W. C. Tait and R. L. Weiher, *Phys. Rev.* **166**, 769 (1968).

<sup>11</sup> Y. Osaka, Y. Imai, and Y. Takeuti, *J. Phys. Soc. Japan* **24**, 236 (1968).

<sup>12</sup> W. C. Tait and R. L. Weiher, *Phys. Rev.* **178**, 1404 (1969).

## Application of the Quantum-Defect Method to Optical Transitions Involving Deep Effective-Mass-Like Impurities in Semiconductors\*

H. BARRY BEBB

*Texas Instruments Incorporated, Dallas, Texas 75222*

(Received 27 January 1969; revised manuscript received 8 May 1969)

Approximate ground-state wave functions for effective-mass impurity centers of arbitrary binding energy are derived by the quantum-defect method and applied to calculate optical absorption and emission processes involving impurities in semiconductors. The dependences of band-impurity and impurity-ionization cross sections on impurity binding energy are calculated and shown to limit to those of the hydrogenic model and Lucovsky's  $\delta$ -function model for shallow and deep impurity centers, respectively. Formulas relating the cross sections to the absorption coefficients and radiative recombination rates are also presented.

### I. INTRODUCTION

THE observed binding energies of effective-mass impurities in semiconductors depend on the chemical species of the impurity ion (e.g., P, As, or Sb donors in silicon or germanium and B, Al, Ga, and In acceptors in silicon).<sup>1</sup> This is contrary to the simple

effective-mass theory which predicts a unique binding energy (for all effective-mass impurities) that depends

\* Work sponsored in part by U. S. Air Force Office of Scientific Research, under Contract No. F44620-67-C-0073.

<sup>1</sup> W. Kohn, in *Solid State Physics*, edited by F. Seitz and D.

Turnbull (Academic Press Inc., New York, 1957), Vol. 5. Kohn briefly discusses the QDM (p. 289) in this connection, but because of an unfortunate error in his asymptotic wave function he does not attain the full significance of the formalism. Kohn records a hydrogenic function with the Bohr radius scaled to the observed energy in the usual way. The correct QD functions possess a rather different form and contain parameters which obviate the necessity of scaling quantities formally specified by the host-crystal properties, e.g., the effective Bohr radius.